The Rho1 GTPase Acts Together With a Vacuolar Glutathione S-Conjugate Transporter to Protect Yeast Cells From Oxidative Stress

Mid Eum Lee,* Komudi Singh,†,1 Jamie Snider,‡ Archana Shenoy,† Christian M. Paumi,§ Igor Stagljar,‡ and Hay-Oak Park*,†,2

†Department of Molecular Genetics and *Molecular Cellular Developmental Biology Program, The Ohio State University, Columbus, Ohio 43210-1292, ‡Donnelly Centre, Department of Biochemistry, Department of Molecular Genetics, University of Toronto, Toronto, Ontario, Canada, and §Graduate Center for Toxicology, University of Kentucky, Lexington, Kentucky 40536

ABSTRACT Maintenance of redox homeostasis is critical for the survival of all aerobic organisms. In the budding yeast *Saccharomyces cerevisiae*, as in other eukaryotes, reactive oxygen species (ROS) are generated during metabolism and upon exposure to environmental stresses. The abnormal production of ROS triggers defense mechanisms to avoid the deleterious consequence of ROS accumulation. Here, we show that the Rho1 GTPase is necessary to confer resistance to oxidants in budding yeast. Temperature-sensitive *rho1* mutants (*rho1^{ts}*) are hypersensitive to oxidants and exhibit high accumulation of ROS even at a semipermissive temperature. Rho1 associates with Ycf1, a vacuolar glutathione S-conjugate transporter, which is important for heavy metal detoxification in yeast. Rho1 and Ycf1 exhibit a two-hybrid interaction with each other and form a bimolecular fluorescent complex on the vacuolar membrane. A fluorescent-based complementation assay suggests that the GTP-bound Rho1 associates with Ycf1 and that their interaction is enhanced upon exposure to hydrogen peroxide. The *rho1^{ts}* mutants also exhibit hypersensitivity to cadmium, while cells carrying a deletion of *YCF1* or mutations in a component of the Pkc1–MAP kinase pathway exhibit little or minor sensitivity to oxidants. We thus propose that Rho1 protects yeast cells from oxidative stress by regulating multiple downstream targets including Ycf1. Since both Rho1 and Ycf1 belong to highly conserved families of proteins, similar mechanisms may exist in other eukaryotes.

CELLS growing aerobically are constantly exposed to ROS, which are generated during normal cellular metabolism and upon exposure to oxidants or metals. Although ROS can regulate several intracellular signaling pathways, these molecules can damage DNAs, proteins, and lipids. Thus maintenance of the intracellular redox state is critical for cellular integrity (Finkel 2003). The abnormal production of ROS leads to the induction of defense mechanisms to avoid the deleterious consequence of ROS accumulation, and oxidative stress occurs when cells cannot efficiently neutralize or eliminate ROS. Several studies in the budding yeast *Saccharomyces cerevisiae*, including genome-wide expression profiling, have identified many genes whose transcripts or protein levels are elevated or repressed in response to oxidants (Morgan *et al.* 1997; Godon *et al.* 1998; Lee *et al.* 1999; Gasch *et al.* 2000; Cohen *et al.* 2002; He and Fassler 2005). These studies have provided insight into the regulatory responses and the oxidative stress response regulons including the two transcription factors Yap1 and Skn7. However, it is not clear how these gene products function to protect cells from oxidative stress. It is also noteworthy that most genes required for resistance to oxidative stress are not induced in response to oxidative stress (Thorpe *et al.* 2004). How cells respond to and recover from oxidative stress is thus largely unknown.

The Rho1 GTPase in budding yeast is involved in a number of different signaling events including the cell wall integrity (CWI) pathway, which is activated by various stresses such as heat shock, hypo-osmotic shock, and nutritional stress (Levin 2005; Park and Bi 2007). Rho1 activates Pkc1, a yeast homolog of mammalian protein kinase C, which participates in activating a MAP kinase (MAPK)-

doi: 10.1534/genetics.111.130724
Manuscript received March 25, 2011; accepted for publication May 17, 2011
Supporting information is available online at http://www.genetics.org/content/suppl/2011/05/30/genetics.111.130724.DC1.
[1]Present address: Department of Neuroscience, Brown University, Providence, RI 02912.
[2]Corresponding author: Department of Molecular Genetics, The Ohio State University, 484 West 12th Ave., Columbus, OH 43210. E-mail: park.294@osu.edu

activation cascade composed of a MEKK (Bck1), a redundant pair of MEKs (Mkk1/2), and a MAPK (Mpk1/Slt2) in response to cell wall stresses (Lee and Levin 1992; Kamada *et al.* 1995; Harrison *et al.* 2004). Rho1 regulates actin organization via the CWI pathway (Delley and Hall 1999; Harrison *et al.* 2001) and by activating the formin Bni1 (Kohno *et al.* 1996; Evangelista *et al.* 1997; Dong *et al.* 2003). Rho1 also regulates 1,3-β-glucan synthesis as a direct regulatory subunit of glucan synthase (encoded by *FKS1* and *GSC2/FKS2*) (Drgonova *et al.* 1996; Qadota *et al.* 1996). A systematic analysis of several high-temperature–sensitive (ts) mutations of *RHO1* led to identification of the distinct functional domains of Rho1—one group of *rho1*^{ts} mutants including *rho1-2* and *rho1-5* is defective in activation of Pkc1, while another group including *rho1-3* is defective in activation of glucan synthase (Saka *et al.* 2001). Rho1 exhibits a two-hybrid interaction with Skn7 (Alberts *et al.* 1998), which regulates the osmotic or oxidative stress response genes (He *et al.* 2009). It is not clear, however, whether Rho1 or the cell integrity MAPK cascade is activated by oxidative stress.

Cells lacking Rom2, a guanine nucleotide exchange factor (GEF) for Rho GTPases, are hypersensitive to oxidants, suggesting possible involvement of Rho1 or other GTPases in the oxidative stress response (Park *et al.* 2005; Vilella *et al.* 2005). Interestingly, another Rho1 GEF, Tus1, was shown to interact with Ycf1 (yeast cadmium factor) by a membrane two-hybrid analysis and co-immunoprecipitation (Paumi *et al.* 2007). Ycf1 is a vacuolar glutathione S-conjugate transporter of the ATP-binding cassette family, and plays an important role in detoxifying metals such as cadmium and arsenite (Li *et al.* 1997). Tus1 stimulates Ycf1 transporter activity in a Rho1-dependent manner (Paumi *et al.* 2007). Numerous studies suggest that metals induce oxidative stress in a variety of cell types (Ercal *et al.* 2001; Valko *et al.* 2005). For example, cadmium is a nonredox metal that has been shown to induce oxidative stress by increasing ROS indirectly in *S. cerevisiae* and neurons (Brennan and Schiestl 1996; López *et al.* 2006; Cuypers *et al.* 2010). These previous studies provided a potential link between Rho1 and Ycf1, but also raised some important questions. Does Ycf1 act upstream of Rho1 or as a downstream effector of Rho1? Does Tus1 activate Rho1 on the vacuolar membrane? Rho1 localizes to the plasma membrane and to other sites including bud tips, the mother-bud neck, and endomembranes (McCaffrey *et al.* 1991; Drgonova *et al.* 1996; Qadota *et al.* 1996; Yoshida *et al.* 2009), while Ycf1 localizes to the vacuolar membrane (Wemmie and Moye-Rowley 1997; Mason and Michaelis 2002). Tus1 localizes to the presumptive bud site in unbudded cells and to the mother-bud neck during cytokinesis (Yoshida *et al.* 2006; Kono *et al.* 2008), but has not been observed on the vacuolar membrane.

These remaining questions led us to investigate a possible role of Rho1 under oxidative stress and the potential interaction between Rho1 and Ycf1 *in vivo*. Here we report that Rho1 is necessary to confer resistance to oxidants and that Rho1 interacts with Ycf1 in a GTP-dependent manner. Our findings thus suggest that Rho1 is involved in reducing ROS in the cell by regulating Ycf1 and other downstream targets.

Materials and Methods

Plasmids and yeast strains

Standard methods of yeast genetics and recombinant DNA manipulation were used (Guthrie and Fink 1991; Ausubel *et al.* 1999). Yeast cells were grown under standard growth conditions at 30° unless otherwise indicated. Yeast strains used in this study are listed in Table 1. Details of plasmid constructions are described in supporting information, File S1, and plasmids used in this study are listed in Table S1.

Plate assays

The sensitivity of the *rho1*^{ts} mutants to paraquat (Sigma-Aldrich) and diethyl maleate (DEM) (Sigma-Aldrich) was determined at 30°, as previously described (Singh *et al.* 2008) with slight modification. The wild-type and *rho1*^{ts} strains were diluted to OD_{600} = 0.4 from mid-to-late logarithmic-phase cultures in YPD and then serially diluted as indicated. These cells were spotted on YPD plates containing 400 μg/ml paraquat, 1 mM DEM, or no oxidant. The plates were incubated at 30° for 2–5 days. To test the sensitivity to H_2O_2, cells were diluted to OD_{600} = 0.8 and then treated with 2 or 3 mM H_2O_2 for 200 min before plating on YPD or SC plates as indicated. The sensitivity to various concentrations of H_2O_2 was tested by halo assays. First, cells from a mid logarithmic-phase culture were diluted to OD_{600} = 0.2. To make a lawn of cells, 200 μl of the diluted culture was spread on YPD or SC plates as indicated. Sterilized filter disks (Whatman filter paper) were placed on the plate and then soaked with 5 μl of H_2O_2 (concentrations ranging from 0.1 to 4 M). The plates were then incubated at 30° for 1–2 days to monitor zones of growth inhibition around the filter disks.

The sensitivity of the *pkc1* mutants (gifts from D. Levin, Johns Hopkins University, Baltimore, MD) to H_2O_2 was tested similarly except that fivefold serial dilutions were made starting from OD_{600} = 1, and cells were plated on SC−Ura containing 1 M sorbitol after treatment with 2 mM H_2O_2 for 200 min or after mock treatment. The *bck1*Δ and *mpk1*Δ mutants (gifts from J. Gray, University of Glasgow, Glasgow, UK) were tested similarly, except plated on the YPD plates. The laboratory wild-type strains exhibited varying degrees of sensitivity to H_2O_2 depending on the background: BY4741 was more sensitive to H_2O_2 compared with other wild-type strains tested (Figure 9, B and C and Figure S1), as previously reported (Higgins *et al.* 2002; Singh *et al.* 2008). The sensitivity of the *ycf1*Δ and *rho1-5* mutants to cadmium was tested by making fivefold serial dilutions starting from OD_{600} = 2, followed by plating on SC containing 30 μM $CdCl_2$. The plates were then incubated at room temperature for 3–7 days.

Table 1 Yeast strains used in this study

Strain		Relevant genotype[a]	Source/comments
NY2284*	α	*ura3 leu2 trp1 his3 ade2 lys2 rho1Δ::HIS3 ade3::RHO1::LEU2*	Guo *et al.* (2001)
NY2285*	**a**	*rho1Δ::HIS3 ade3::rho1-2^{E45V}::LEU2*	Guo *et al.* (2001)
NY2286*	α	*rho1Δ::HIS3 ade3::rho1-3^{L60P}::LEU2*	Guo *et al.* (2001)
NY2287*	**a**	*rho1Δ::HIS3 ade3::rho1-5^{G121C}::LEU2*	Guo *et al.* (2001)
HPY1710*	α	*YCF1-VN::kanMX6*	See text
HPY1737*	α	*tus1Δ::TRP1 YCF1-VN::kanMX6*	See text
HPY1738*	α	*ycf1Δ::kanMX4*	See text
HPY1739*	**a**	*rho1Δ::HIS3 ade3::rho1-5^{G121C}::LEU2 ycf1Δ::kanMX4*	See text
HPY1574*	α	*RHO1::GFP-RHO1-URA3*	Derived from NY2284[b]
HPY1730*	**a**	*rho1-2::GFP-RHO1-URA3*	Derived from NY2285[b]
HPY1731*	α	*rho1-3::GFP-RHO1-URA3*	Derived from NY2286[b]
HPY1732*	**a**	*rho1-5::GFP-RHO1-URA3*	Derived from NY2287[b]
HPY1955*	α	*YCF1-GFP::TRP1*	See text
EG123#	α	*ura3-52 leu2-3,112 trp1-1 his4 can1*	Same as HPY11, Park *et al.* (1993)
DL106#	α	*pkc1Δ::LEU2* YCp50-PKC1	Levin and Bartlett-Heubusch (1992)
DL511#	α	*pkc1Δ::LEU2* YCp50-pkc1-1	Levin and Bartlett-Heubusch (1992)
DL506#	α	*pkc1Δ::LEU2* YCp50-pkc1-2	Levin and Bartlett-Heubusch (1992)
DL504#	α	*pkc1Δ::LEU2* YCp50-pkc1-3	Levin and Bartlett-Heubusch (1992)
DL253#	α	*bck1Δ::URA3*	Lee and Levin (1992)
JVG216#	**a**	*mpk1Δ::TRP1*	Krause and Gray (2002)
BY4741@	**a**	*his3Δ1 leu2Δ0 met15Δ0 ura3Δ0*	Open Biosystems
HPY1904@	**a**	*ycf1Δ::kanMX4*	Open Biosystems
HPY1905@	**a**	*ybt1Δ::kanMX4*	Open Biosystems
HPY1906@	**a**	*bpt1Δ::kanMX4*	Open Biosystems
THY AP4^	**a**	*leu2, ura3, trp1::(lexAop)-lacZ (lexAop)-HIS3 (lexAop)-ADE2*	Obrdlik *et al.* (2004)
YCF1–CT^	**a**	*YCF1-Cub-LexA-VP16 KanMX*	Derived from THY AP4
ArBT–CT^	**a**	*SHO1::MFαSS-CD4tm-Cub-LexA-VP16 KanMX*	Derived from THY AP4
YCF1–CT ΔT^	**a**	*YCF1-Cub-LexA-VP16 KanMX tus1Δ::NatR*	Derived from THY AP4
ArBT–CT ΔT^	**a**	*SHO1::MFαSS-CD4tm-Cub-LexA-VP16 KanMX tus1Δ::NatR*	Derived from THY AP4

[a] Strains marked with * are isogenic to NY2284, except as indicated; strains marked with @ are isogenic to BY4741, except as indicated; strains marked with # are isogenic to EG123 (Park *et al.* 1993), except as indicated; strains marked with ^ are isogenic to THY AP4 except as indicated; and the background of the strains marked with * and @ is S288C.

[b] pRS306–GFP–RHO1 (pHP1699) was integrated into the *RHO1* locus after digestion with *Bgl*II.

Determination of ROS accumulation

ROS accumulation was monitored indirectly by fluorescence microscopy and flow cytometry, as previously described (Singh *et al.* 2008) with slight modifications. The *rho1^{ts}* mutant cells, grown overnight in YPD at room temperature, were diluted threefold and grown for 3 additional hours. These cells were incubated with dihydrorhodamine 123 (DHR) (Sigma Chemical) for 2 hr at 30°, along with or without 1 mM H_2O_2, and then analyzed by fluorescence microscopy with the FITC filter. For flow cytometry analysis, cells were grown similarly, except that the cultures were diluted to OD_{600} = 0.6 before adding DHR at 30°. Half of the cells were shifted to 37° for 2 hr, while the remaining cells were maintained at 30°. Both cultures were then analyzed with the FACSCalibur (Becton Dickinson) with λ_{ex} = 488 nm excitation and FL1 (530/30 BP) filter.

Integrated membrane yeast two-hybrid analysis

Integrated membrane yeast two-hybrid (iMYTH) assays and construct generation were performed as previously described (Paumi *et al.* 2007; Snider *et al.* 2010). Construction details of the NubG fusions of Rho1 and the *TUS1* deletion strains are provided in File S1. THY AP4 MYTH reporter strains, which harbor chromosomally encoded Ycf1 or unrelated control bait fused to the Cub–LexA–VP16 tag at the C terminus, were transformed with plasmids encoding NubG-tagged Rho1 or control constructs. Cells were plated on SC−Trp as a control to show the presence of prey plasmid and comparative growth between strains. The bait–prey interaction was monitored on SC−Trp−Ade−His containing X-Gal.

Fluorescence microscopy and bimolecular fluorescence complementation

Image acquisition of GFP–Rho1 was carried out essentially as previously described (Kang *et al.* 2001) using a Nikon E800 microscope (Nikon, Tokyo, Japan) fitted with a 100× oil-immersion objective (N.A. = 1.30), a Uniblitz electronic shutter, a Prior *Z*-axis drive, and a Hamamatsu Orca ER cooled charge-coupled device. A series of optical sections was captured at 0.3-μm intervals using Slidebook software (Intelligent Imaging Innovations, Denver, CO) by exposing for 1 sec. Cells were treated with 1–2 mM H_2O_2 for 2–4 hr or mock treated, where indicated, before imaging.

Bimolecular fluorescence complementation (BiFC) assays were performed as previously described (Singh *et al.* 2008; Kang *et al.* 2010) with slight modifications. Rho1 was fused

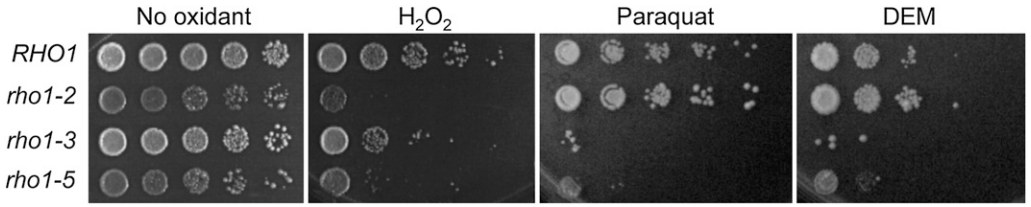

Figure 1 The *rho1^{ts}* mutants are hypersensitive to oxidants. Five-fold serial dilutions (from left to right) of wild-type (NY2284), *rho1-2* (NY2285), *rho1-3* (NY2286), and *rho1-5* (NY2287) cells were grown at 30° for 2–4 days on YPD after treating with 3 mM H_2O_2 for 200 min or mock treatment, and on YPD containing 400 μg/ml of paraquat or 1 mM DEM.

to the C-terminal fragment of YFP (YFP^C) at its N terminus and was expressed from a CEN or 2μ plasmid (where indicated). Ycf1 was fused to the N-terminal fragment of Venus (VN), a variant YFP (Nagai *et al.* 2002), at its C terminus, and was expressed from its chromosomal locus (see File S1 for details of the plasmid and strain construction). To monitor BiFC signals, a single optical section was captured using the YFP filter by exposing cells to UV for 8 sec. Imaging and image processing were performed under identical conditions for all BiFC assays. Where indicated, the vacuolar membrane was visualized by staining cells with FM4-64 for 30 min at room temperature as previously described (Vida and Emr 1995). Localization pattern and pixel intensity of the bimolecular fluorescent complex and Ycf1–GFP were analyzed by counting at least 100 cells per experiment from three independent experiments. Image analysis and processing were performed with ImageJ software, and the data are presented as mean ± SD. Statistical significance was determined using Student's *t*-test.

Results

rho1^{ts} mutants are hypersensitive to various oxidants

To determine whether *RHO1* regulates the cellular response to oxidative stress, we examined sensitivity of the *rho1^{ts}* mutants, *rho1-2*, *rho1-3*, and *rho1-5*, to oxidants including paraquat, diethyl maleate (DEM), and hydrogen peroxide (H_2O_2). Paraquat is a superoxide-generating agent (Cochemé and Murphy 2008), and DEM is a thiol-specific oxidant that depletes glutathione in the cell (Nguyên-Nhu and Knoops 2002). Both drugs increase intracellular ROS levels. Hydrogen peroxide is in itself poorly reactive but can be readily converted to the highly reactive hydroxyl radical upon exposure to UV or by interaction with metal ions (Valko *et al.* 2005). When serial dilutions of these *rho1* mutants were spotted on rich plates containing paraquat or DEM at 30°, *rho1-3* and *rho1-5* were hypersensitive to these oxidants compared to wild type, while *rho1-2* exhibited little sensitivity to these drugs (Figure 1). These *rho1* mutants also exhibited sensitivity to H_2O_2 to different extents, with *rho1-2* and *rho1-5* being particularly hypersensitive to H_2O_2 (Figure 1 and Figure S1A). Taken together, these results suggest that Rho1 is necessary to confer resistance to oxidants.

Cells of the rho1^{ts} mutants exhibit high ROS accumulation

To test whether the hypersensitivity of the *rho1^{ts}* mutants to oxidants resulted from its specific defect in maintaining cellular redox balance rather than general sickness, we indirectly monitored the intracellular ROS level using DHR, which becomes fluorescent rhodamine 123 upon oxidation (Herker *et al.* 2004). When these cells were examined by flow cytometry after adding DHR, we found that a high level of ROS was present in the *rho1* mutants even when they were grown at the semipermissive temperature of 30°, but not in wild-type cells (Figure 2A). A higher percentage of the *rho1* mutant cells exhibited increased fluorescence upon shifting the cultures to 37° (Figure 2A). When the *rho1-5* mutant was examined under the fluorescence microscope, high fluorescence was observed in the cytoplasm at 30° and in an even higher percentage of the cells after exposure to H_2O_2 (Figure 2B). These results thus suggest that ROS were not efficiently removed in the cytoplasm of the *rho1^{ts}* mutants.

The Pkc1–MAPK pathway may play a minor role under oxidative stress

What is the downstream target of Rho1 that is involved in the oxidative stress response? Since *rho1-2* and *rho1-5*, which are defective in activating Pkc1 (Saka *et al.* 2001), were hypersensitive to H_2O_2, we wondered whether Rho1 regulates the Pkc1–MAPK pathway under oxidative stress. We thus examined the sensitivity of *pkc1^{ts}* mutants to H_2O_2. A *pkc1*Δ mutant with a plasmid carrying the *pkc1* allele, *pkc1-1*, *pkc1-2*, or *pkc1-3*, exhibited slight sensitivity to H_2O_2 at 25–33° on the plate containing sorbitol as an osmotic stabilizer and cell wall protective agent (Figure 3A). Similarly, we found that cells lacking the downstream components of Pkc1, *bck1*Δ and *mpk1/slt2*Δ, were also slightly more sensitive to H_2O_2 than wild type (Figure 3B), suggesting that the Pkc1–MAPK pathway may play a minor role in recovery from oxidative stress.

Rho1 interacts with Ycf1 in vivo

Since the phenotype of the *pkc1* or *mpk1* mutant upon exposure to H_2O_2 was much milder than that of *rho1* mutants, Rho1 might regulate another downstream target involved in the oxidative stress response. Because Tus1 interacts with

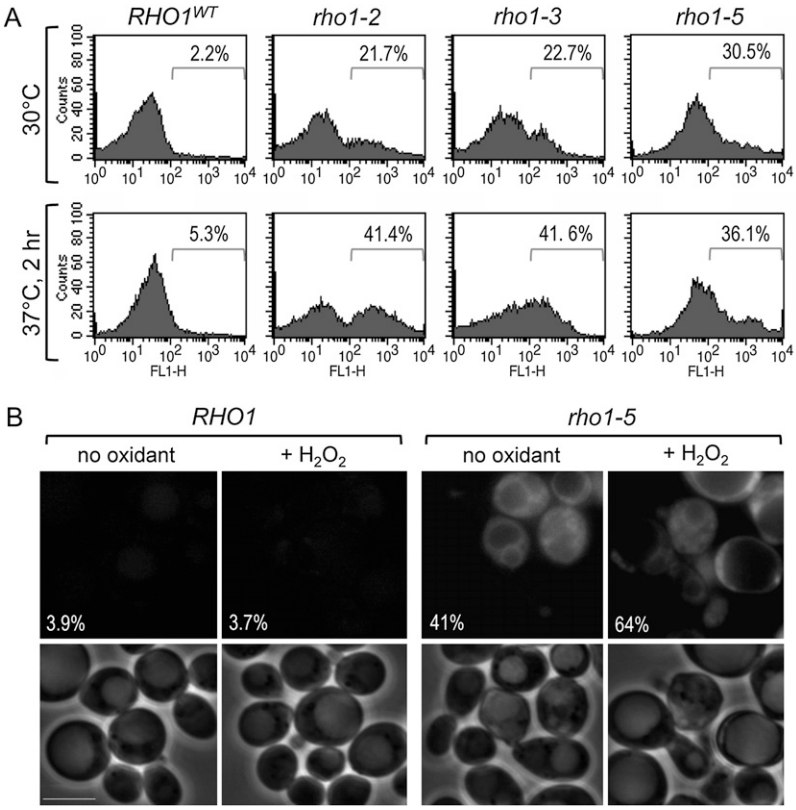

Figure 2 The *rho1*^{ts} mutants exhibit a high level of ROS accumulation. (A) FACS analysis of wild-type (NY2284) and *rho1* mutant cells (NY2285–NY2287) grown at 30° or shifted to 37° for 2 hr and stained with DHR. Histograms of single representative experiment are shown from three independent experiments. n = 10,000 for each sample. (B) Cells of wild type and *rho1-5* were grown at 30° and visualized by fluorescence microscopy after staining with DHR during a 2-hr incubation with or without 1 mM H_2O_2. Fluorescence (top) and phase contrast (bottom) images of representative cells are shown from three independent experiments (n = 450–650 cells for each sample), and the average percentages of the cells with detectable fluorescence are shown. Bars, 5 μm.

Ycf1 (Paumi *et al.* 2007), we wondered whether Ycf1 might be such a Rho1 target. We hypothesized that dysfunction of Ycf1 in the *rho1*^{ts} mutants might lead to increased ROS accumulation in the cytoplasm. To test whether Rho1 interacts with Ycf1 *in vivo*, first we performed an integrated split-ubiquitin membrane yeast two-hybrid (iMYTH) analysis (Snider *et al.* 2010). The reporter strains, which harbored chromosomally encoded Ycf1 or unrelated control bait fused to Cub–LexA–VP16, were transformed with a plasmid encoding NubG-tagged Rho1 or a control construct (see *Materials and Methods* and File S1) and then plated onto SC−Trp (Figure 4A, a–f). The bait–prey interactions were then determined by monitoring growth and β-galactosidase expression on SC plates lacking Trp, Ade, and His but containing X-Gal (Figure 4A, g–l). Both Ycf1–Cub–LexA–VP16 and the control bait strains grew and exhibited blue color in the presence of the positive control prey Ost1–NubI (Figure 4A, g and h, top row) but not in the presence of the non-interacting control prey Ost1–NubG (Figure 4A, g and h, bottom row). The Ycf1 strain, but not the control bait, exhibited robust growth and blue color in the presence of NubG–Rho1 (Figure 4A, i and j, top row). In contrast, the reporter strain expressing Rho1 with the NubG tag at its C terminus (Rho1–NubG) or the control bait strain did not show such growth and blue coloration (Figure 4A, i and j, bottom row). This absence of interaction is likely due to the C-terminal NubG tag preventing proper membrane targeting of Rho1. Taken together, these data indicate that Rho1 interacts specifically with Ycf1 *in vivo*.

Next, we performed a BiFC assay to monitor the Rho1–Ycf1 interaction *in vivo*. This assay allows visualization of protein–protein associations in live cells by monitoring YFP fluorescence, which appears when truncated YFP fragments (YFP^N and YFP^C) are brought together by association of the two proteins fused to them (Hu *et al.* 2002). We expressed YFP^C–Rho1 from a low-copy plasmid in a strain expressing

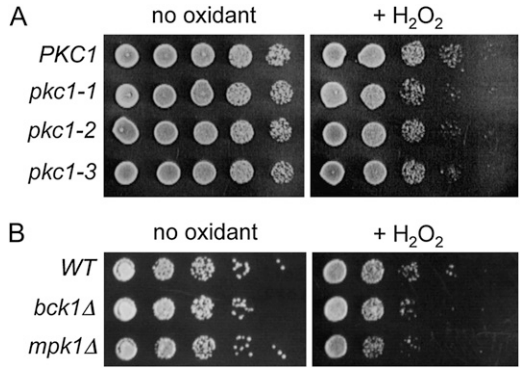

Figure 3 The *pkc1* mutants and cells lacking downstream components of Pkc1 are mildly sensitive to H_2O_2. (A) Fivefold serial dilutions (from left to right starting from OD_{600} = 1) of *pkc1*Δ mutant carrying YCp–PKC1 (DL106), YCp–pkc1-1 (DL511), YCp–pkc1-2 (DL506), and YCp–pkc1-3 (DL504) were grown at 25, 30, and 33° for 2–4 days on SC−Ura plates containing 1 M sorbitol after treatment with 2 mM H_2O_2 for 200 min or mock treatment. The results were about the same at all temperatures tested, and only the plate at 30° is shown. (B) Cells of *bck1*Δ (DL253) and *mpk1*Δ (JVG216) mutants were treated similarly, except plated on YPD plates at 30°.

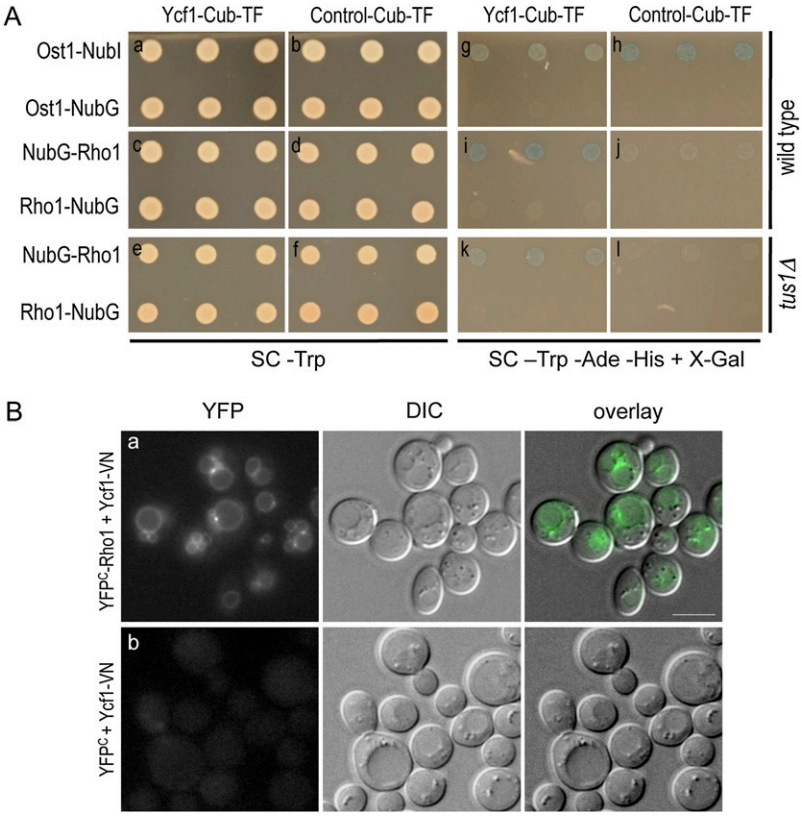

Figure 4 Rho1 associates with Ycf1 *in vivo*. (A) iMYTH assays to determine the Rho1–Ycf1 interaction. THY AP4 MYTH reporter strains, expressing either C-terminally Cub–LexA–VP16 tagged Ycf1 or unrelated control bait, carry NubG-tagged Rho1 or other control plasmid as indicated. These cells were plated on SC−Trp to show the presence of prey plasmid and comparative growth among strains (a–f) and on SC−Trp−Ade−His containing X-Gal to monitor bait–prey interactions (g–l). Strains used for each panel are: YCF1–CT (a, c, g, and i); ArBT–CT (b, d, h, and j); YCF1–CT ΔT (e and k); and ArBT–CT ΔT (f and l). (B) BiFC assays were performed in wild-type cells (HPY1710), which express Ycf1–VN from its chromosomal locus and carry pRS316–YFP^C–RHO1 (a) or YCp50–YFP^C (b). Cells were grown in SC−Ura at 30°. Images were captured with the YFP filter for 8-sec exposures. Fluorescent images (YFP), DIC images (DIC), and fluorescent images overlaid with the DIC images (overlay) are shown for the representative cells. Bars, 5 μm. See Figure 5B for quantitation of the localization pattern of the Rho1–Ycf1 bimolecular fluorescent complex.

Ycf1–VN from the chromosome (*Materials and Methods*). Ycf1–VN and YFP^C–Rho1 were partially functional on the basis of complementation of cadmium sensitivity of *ycf1Δ* and H_2O_2 sensitivity of *rho1–5*, respectively (Figure S2, A and B). When these fusion proteins were coexpressed, the majority of cells exhibited a strong YFP signal on the vacuolar membrane (Figure 4B, a). Some of these cells also showed one or two fluorescent puncta at the sites where two vacuolar lobes overlapped (see Figure 5B for quantitation). In contrast, no cells exhibited detectable fluorescence in a control strain that coexpressed Ycf1–VN and YFP^C (without a Rho1 fusion) (Figure 4B, b). These results thus indicate that Rho1 interacts directly or closely associates with Ycf1 *in vivo*.

Association of Rho1 with Ycf1 is likely to depend on its GTP-bound state

Next, to determine whether Rho1 interacts with Ycf1 in a GTP-dependent manner, we expressed YFP^C–Rho1^{Q68L} and YFP^C–Rho1^{T24N}, which are expected to be in the GTP- and GDP-locked state *in vivo*, respectively (Nonaka *et al.* 1995), in the *YCF1–VN* strain. Cells coexpressing YFP^C–Rho1^{Q68L} and Ycf1–VN exhibited BiFC signals (Figures 5A, a), although the percentage of cells with little signal was increased (see *Discussion*). In contrast, cells coexpressing YFP^C–Rho1^{T24N} and Ycf1–VN showed little fluorescence (Figure 5A, b). The Rho1^{Q68L}–Ycf1 BiFC signal was often observed on the vacuolar membrane and in several puncta on the vacuolar membrane (see Figure 5B for quantitation). The YFP signals in these cells appeared less discrete than those observed in the cells coexpressing YFP^C–Rho1 and Ycf1–VN. This is likely due to the vacuolar shape in cells expressing YFP^C–Rho1^{Q68L}, as visualized by differential interference contrast (DIC) microscopy. Staining with FM4-64 also revealed different morphology of the vacuolar membrane in these cells (Figure S3). Despite these differences, these data thus suggest that Rho1–GTP interacts with Ycf1.

We hypothesized that the formation of the Rho1–Ycf1 complex would depend on Tus1, which converts Rho1 to the GTP-bound state. To test this idea, we performed BiFC assays in a strain deleted for *TUS1*. When the interaction between YFP^C–Rho1 and Ycf1–VN was examined in the *tus1Δ* mutant, fewer cells indeed show a detectable BiFC signal (compare Figure 5A, c to Figure 4B, a). However, a significant percentage of *tus1Δ* cells still showed the Rho1–Ycf1 bimolecular fluorescent complex (Figure 5B). When fluorescence of these cells with positive BiFC signals was compared, the mean pixel intensity of the vacuolar membrane was about the same in wild-type and *tus1Δ* cells (Figure 5C). Consistent with the BiFC results, iMYTH analysis in a *tus1Δ* reporter strain indicated that Rho1 interacts with Ycf1 specifically even in the absence of *TUS1* (Figure 4A, k and l). It is thus likely that another GEF compensates for the loss of Tus1 in *tus1Δ* cells. The Rho1^{Q68L}–Ycf1 bimolecular fluorescent complex was also observed in *tus1Δ* cells (Figure 5A, d and 5B), and the total fluorescence intensity in individual cells was not statistically different between wild type and the *tus1Δ* mutant.

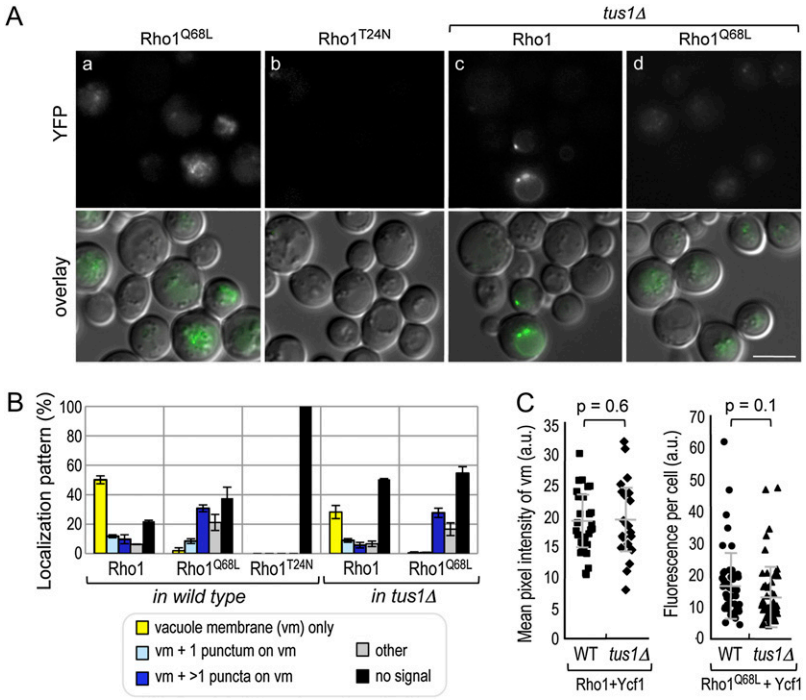

Figure 5 The Rho1–Ycf1 bimolecular fluorescent complex formation is dependent on the GTP-bound state of Rho1 *in vivo*. (A) BiFC assays were performed in the *YCF1–VN* strain (HPY1710), which carries (a) pRS316–YFP^{C}–RHO1^{Q68L} or (b) pRS316–YFP^{C}–RHO1^{T24N}, and the *YCF1–VN tus1*Δ strain (HPY1737), which carries (c) pRS316–YFP^{C}–RHO1 or (d) pRS316–YFP^{C}–RHO1^{Q68L}. Cells were grown in SC−Ura at 30°. Images were captured, processed, and presented as in Figure 4B. Bar, 5 μm. (B) Localization pattern of the Rho1–Ycf1 bimolecular fluorescent complex: the vacuolar membrane (vm) only; the vm and a punctum on the vm; the vm and a few puncta on the vm; and others, which are mixed patterns with diffuse signal often enriched in the vacuole. Localization pattern of bimolecular fluorescent complex was quantitated from three independent experiments (n = 300–400), and mean (%) ± SD are shown. (C, left) Mean pixel intensity of the vacuolar membrane of each individual cell was plotted and quantified using ImageJ software: WT (HPY1710 with pRS316–YFP^{C}–RHO1), 18.7 ± 5.0 (in arbitrary units, a.u.) and *tus1*Δ (HPY1737 with pRS316–YFP^{C}–RHO1), 19.5 ± 6.3 (in a.u.) (P = 0.6). (Right) Fluorescence intensity of each individual cell was analyzed: WT (HPY1710 with pRS316–YFP^{C}–RHO1^{Q68L}), 16.9 ± 10.9 (in a.u.) and *tus1*Δ (HPY1737 with pRS316–YFP^{C}–RHO1^{Q68L}), 13.5 ± 9.4 (in a.u.) (P = 0.1).

The Rho1–Ycf1 interaction may increase upon exposure to H_2O_2

Since Ycf1 formed a bimolecular fluorescent complex with the GTP-locked Rho1 but not with the GDP-locked Rho1, Rho1 might be activated upon exposure to oxidants and thus form more Rho1–Ycf1 bimolecular fluorescent complex. To test the idea, we performed BiFC assays in cells coexpressing Ycf1–VN and YFP^{C}–Rho1 after treatment with H_2O_2. While the BiFC signals appeared on the vacuolar membrane similar to those in untreated cells, more cells showed several puncta with stronger fluorescence on the vacuolar membrane (Figure 6A, a). This is particularly evident in cells expressing YFP^{C}–Rho1 from a multicopy plasmid after exposure to H_2O_2 (Figure 6B, b and 6D). Quantification of fluorescence intensity of these cells indeed indicated that the pixel intensity of individual cells and in each punctum increased from 9.57 ± 5.4 to 15.13 ± 9.9 (in arbitrary units, a.u.; P = 0.0002) and from 0.64 ± 0.1 to 0.94 ± 0.5 (P = 0.002), respectively, after H_2O_2 treatment (Figure 6C). Despite the cell-to-cell variation, these differences are statistically significant. Cells expressing Ycf1–VN and YFP^{C} (without the Rho1 fusion), however, did not show such signal after H_2O_2 treatment (Figure 6A, b), suggesting that these dots represent the Rho1–Ycf1 bimolecular fluorescent complex rather than any other endogenous proteins that became fluorescent after H_2O_2 treatment. The fluorescence signal was occasionally observed in the vacuolar lumen in some cells upon exposure to H_2O_2, which might result from mistargeting of the bimolecular fluorescent complex under oxidative stress. Taken together, these results suggest that the interaction between Rho1 and Ycf1 increased after H_2O_2 exposure (see *Discussion*).

Localization of GFP–Rho1 remains similar, while the Ycf1–GFP level is elevated after exposure to H_2O_2

We questioned whether localization of the Rho1–Ycf1 bimolecular fluorescent complex indeed indicates the sites at which these two proteins interact with each other *in vivo* and how localization of Rho1 and Ycf1 is affected upon exposure to H_2O_2. We thus examined localization of Rho1 before and after exposure to H_2O_2 using a strain, which expressed GFP–Rho1 under its native promoter from the chromosome. Expression of GFP–Rho1 in *rho1^{ts}* mutants restored the resistance to H_2O_2, although less efficiently than wild type (compare Figure S2C to Figure 1), indicating that GFP–Rho1 was partially functional. GFP–Rho1 localized to the plasma membrane and to the sites of polarized growth as well as to the vacuolar membrane as expected (Figure 7a). This localization pattern of GFP–Rho1 remained similar after exposure to H_2O_2, although diffuse signals were also occasionally seen in the vacuolar lumen in some cells (Figure 7b). Thus, Rho1 is likely to interact with Ycf1 on the vacuolar membrane where the two proteins colocalize, and localization of GFP–Rho1 is mostly unaffected by H_2O_2.

We next examined localization of Ycf1–GFP, which was expressed from the *YCF1* chromosomal locus. While Ycf1–GFP localized to the vacuolar membrane similarly before and after exposure to H_2O_2 (Figure 8A), the mean pixel intensity of the vacuolar membrane increased from 59.2 ± 18.8 to 71.6 ± 30.1 (in a.u.) after H_2O_2 treatment (Figure 8B). This increase is statistically significant (P = 0.03), albeit rather heterogeneous among individual cells, suggesting that the Ycf1 level is elevated under oxidative stress.

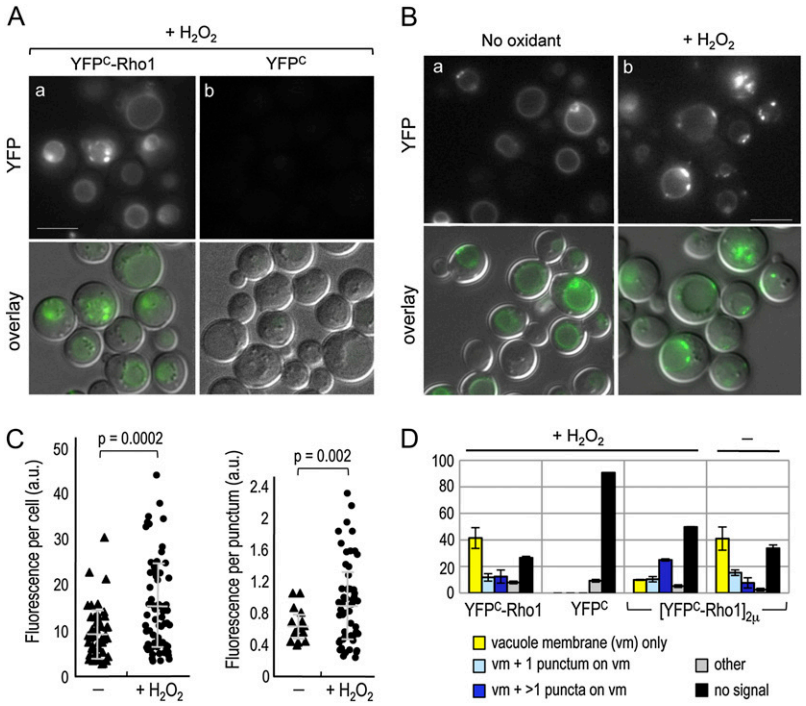

Figure 6 The Rho1–Ycf1 bimolecular fluorescent complex formation after exposure to H_2O_2. (A) BiFC assays were performed in the *YCF1–VN* strain (HPY1710), carrying (a) pRS316–YFP^C–RHO1 or (b) YCp–YFP^C (pHP1730). Cells were grown in SC−Ura at 30° and incubated with 2 mM H_2O_2 for 2 hr before imaging. Images were captured, analyzed, and presented as in Figure 4B. Bar, 5 μm. (B) BiFC assays were performed in HPY1710, carrying pRS426–YFP^C–RHO1. Cells were grown in SC−Ura at 30° and incubated with 2 mM H_2O_2 for 4 hr (+H_2O_2) or mock treated (no oxidant) before imaging. Images were captured, analyzed, and presented as in Figure 4B. Bar, 5 μm. (C, left) Fluorescence intensity of individual cells of HPY1710 with pRS426–YFP^C–RHO1 was plotted and quantified using ImageJ software: pixel intensity in untreated cells, 9.57 ± 5.4 (in a.u.) and in cells treated with 2 mM H_2O_2 for 4 hr, 15.1 ± 9.9 (in a.u.) (P = 0.0002). (C, right) Fluorescence intensity of each punctum in HPY1710 with pRS426–YFP^C–RHO1 was analyzed similarly: pixel intensity in untreated cells, 0.64 ± 0.1 (in a.u.) and in cells treated with 2 mM H_2O_2 for 4 hr, 0.94 ± 0.5 (in a.u.) (P = 0.002). (D) Localization pattern of the Rho1–Ycf1 bimolecular fluorescent complex was analyzed as in Figure 5B from strains HPY1710 with pRS316–YFP^C–RHO1, YCp–YFP^C, or pRS426–YFP^C–RHO1 after treatment with H_2O_2 for 4 hr and HPY1710 with pRS426–YFP^C–RHO1 after mock treatment. Data are from three independent experiments (n = 300–400), and mean (%) ± SD are shown.

rho1^{ts} mutants are hypersensitive to cadmium, while an ycf1Δ mutant exhibits slight sensitivity to H_2O_2

On the basis of our data described above, together with previous observations (Paumi *et al.* 2007), we hypothesized that Rho1 activates Ycf1. If this were the case, we would expect a *rho1^{ts}* mutant to be hypersensitive to cadmium and an *ycf1Δ* mutant to be sensitive to H_2O_2. To test these predictions, we examined the sensitivity of the *rho1-2*, *rho1-3*, and *rho1-5* mutants to cadmium. Indeed, these *rho1* mutants were sensitive to $CdCl_2$ to different extents (Figure 9A), and the pattern of the differential sensitivity was similar to those seen for paraquat and DEM (Figure 1).

Next, we examined the H_2O_2 sensitivity of an *ycf1Δ* mutant in two strain backgrounds. A *ycf1Δ* mutant exhibited similar sensitivity to H_2O_2 compared to each isogenic wild-type strain (Figure 9, B and C) and the mutants lacking other vacuolar ABC transporters, *ybt1Δ* and *bpt1Δ* (Figure 9B). At relatively higher H_2O_2 concentrations, however, *ycf1Δ* was slightly more sensitive to H_2O_2 than wild type (Figure S1B). In addition, when the *rho1-5* and *ycf1Δ* mutations were combined, the double mutant was slightly more sensitive to H_2O_2 than *rho1-5* (Figure 9C). Taken together, these observations thus suggest that Ycf1 contributes to resistance to both metals and oxidants, although loss of *YCF1* alone does not result in hypersensitivity to H_2O_2. These results also indicate that other targets of Rho1 as well as Ycf1 are likely to modulate cytoplasmic ROS level, since *rho1^{ts}* was much more sensitive to H_2O_2 than *ycf1Δ* (see *Discussion*).

Discussion

Rho1 activates the "cell integrity" MAPK pathway in response to various stresses (Levin 2005), but it has not been clear whether Rho1 or any other component of the MAPK pathway is also involved in the oxidative stress response. Although the Rho1 GEF, Tus1, interacts with Ycf1 (Paumi *et al.* 2007), it remained unclear whether Ycf1 functions upstream or as a target of Rho1. The studies reported here now clarify some of these outstanding issues and uncover a heterogeneous and complex cellular response to oxidative stress.

Temperature-sensitive *rho1* mutants were hypersensitive to oxidants and exhibited an elevated level of ROS accumulation in the cytoplasm. A membrane two-hybrid analysis and

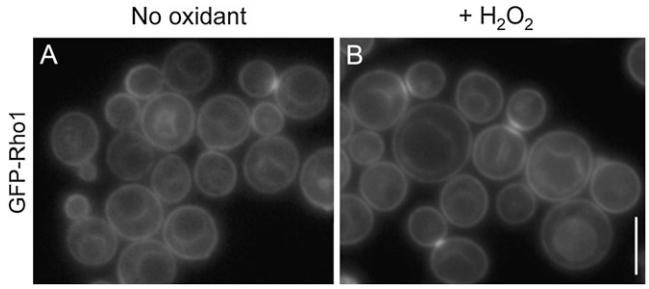

Figure 7 Localization of GFP–Rho1, expressed from the chromosome, was examined in wild-type cells (HPY1574), grown in SC−Ura at 30°, (A) before and (B) after exposure to 2 mM H_2O_2 for 2 hr. A series of Z sections was captured with the GFP filter and a single, representative Z section is shown. Bar, 5 μm.

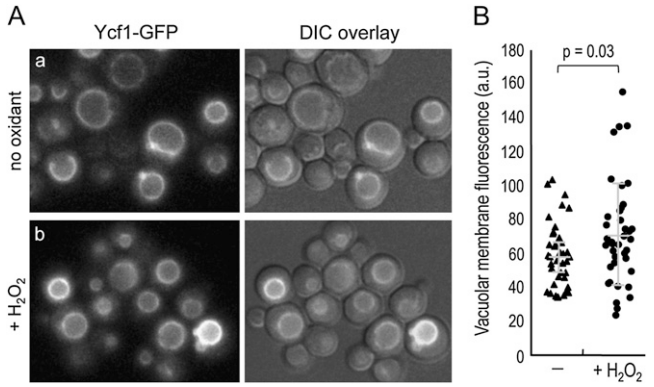

Figure 8 (A) Localization of Ycf1–GFP was examined in the *YCF1–GFP* strain (HPY1955), grown in SC−Trp at 30°, before and after exposure to 2 mM H_2O_2 for 2 hr. A series of *Z* sections was captured with the GFP filter and a single, representative *Z* section is shown. (B) Fluorescence intensity of the vacuolar membrane was plotted and quantified using ImageJ software: pixel intensity in untreated cells, 59.2 ± 18.8 (in a.u.); and in cells treated with H_2O_2, 71.6 ± 30.1 (in a.u.) ($P = 0.03$).

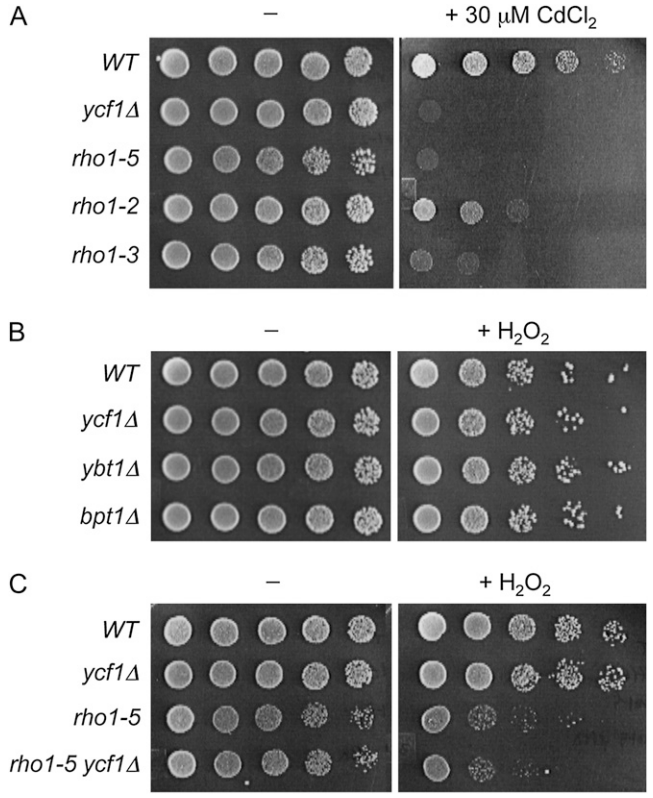

Figure 9 *rho1^{ts}* mutants are hypersensitive to cadmium while *ycf1*Δ mutant are slightly sensitive to H_2O_2. (A) Fivefold serial dilutions (from left to right, starting from $OD_{600} = 2$) of wild-type (NY2284), *ycf1*Δ (HPY1738), *rho1-5* (NY2287), *rho1-2* (NY2285), and *rho1-3* (NY2286) strains, all of which are in the isogenic background, were grown on SC or SC plate containing 30 μM $CdCl_2$ at room temperature for 4 days (−) or 7 days (+30 μM $CdCl_2$). (B) Fivefold serial dilutions (from left to right, starting from $OD_{600} = 1$) of wild type (BY4741) and isogenic deletion mutants of vacuolar transporters (*ycf1*Δ, *ybt1*Δ, and *bpt1*Δ) were treated with 2 mM H_2O_2 or mock treated, spotted on SC plates, and incubated at 30° for 2 days. (C) Fivefold serial dilutions (from left to right, starting from $OD_{600} = 1$) of wild type (NY2284), *ycf1*Δ (HPY1738), *rho1-5* (NY2287), and *rho1-5 ycf1Δ* (HPY1739) were treated as in Figure 9B.

a fluorescence-based complementation assay demonstrate that Rho1 interacts with Ycf1 *in vivo*, likely in its GTP-bound state (see below). Together with the previous finding that Ycf1 activity depends on Rho1 (Paumi *et al.* 2007), our findings thus suggest that Rho1 activates Ycf1 to regulate the redox balance in the cell. Neither the *ycf1*Δ nor the *pkc1^{ts}* mutants, however, exhibited such hypersensitivity to H_2O_2, suggesting that Rho1 regulates the oxidative stress response probably through multiple downstream targets. We observed high cell-to-cell variation in cellular response to oxidative stress, including the levels of Ycf1, the Rho1–Ycf1 bimolecular fluorescent complex, and ROS accumulation upon exposure to H_2O_2. This is likely due to a different age and physiological state of individual cells. In fact, cellular age in eukaryotes is a particularly well-known determinant of heterogeneous resistance to oxidative burden (Avery 2006).

Cells expressing the GTP-locked Rho1^{Q68L} showed a positive BiFC signal, whereas cells expressing the GDP-locked Rho1^{T24N} did not, suggesting that Rho1–GTP interacts with Ycf1. It is thus likely that Ycf1 is a downstream target of Rho1. The localization pattern of the Rho1^{Q68L}–Ycf1 bimolecular fluorescent complex appeared different from that of Rho1, reflecting the different vacuole morphology in cells expressing Rho1^{Q68L} (Figure S3). Indeed, Rho1 is also involved in vacuole membrane fusion (Eitzen *et al.* 2001; Logan *et al.* 2010). It might also correspond to the intrinsic difference between the GTP-locked Rho1 and the GTP-bound Rho1, which can cycle back to the GDP-bound state, with respect to their association with Ycf1. Although fewer cells exhibited BiFC signals with Rho1^{Q68L} than with the wild type, this is likely due to the sickness of cells expressing Rho1^{Q68L} (Nonaka *et al.* 1995), which might have caused loss of the YFP^{C}–Rho1^{Q68L} plasmid in some cells. Since Tus1 also interacts with Ycf1 (Paumi *et al.* 2007), Tus1 may facilitate the interaction between Rho1 and Ycf1 on the vacuolar membrane as well as the GDP–GTP exchange on Rho1. We were, however, unable to observe convincing Tus1 localization to the vacuolar membrane before or after exposure to H_2O_2, likely due to transient localization or a very weak signal of Tus1–GFP. Rho1 still interacted with Ycf1 in *tus1*Δ cells, albeit less efficiently, suggesting that another Rho1 GEF substitutes Tus1 function in a *tus1*Δ mutant.

The Rho1–Ycf1 bimolecular fluorescent complex was observed on the vacuolar membrane and occasionally as one or two dots on the vacuolar membrane. Although the exact nature of these puncta remains unclear, both patterns of the BiFC signals were dependent on Rho1 and Ycf1. Interestingly, the number of these puncta on the vacuolar membrane and their pixel intensity increased after exposure to H_2O_2, suggesting an increased interaction between Rho1 and Ycf1 upon exposure to H_2O_2. This might be due to the activation of Rho1 as well as elevation of the Ycf1 protein level upon exposure to H_2O_2 (Figure 8), consistent with the fact that Yap1 regulates the expression of *YCF1* (Sharma

et al. 2002). It is also possible that these puncta reflect the coalescence of the Rho1–Ycf1 bimolecular fluorescent complexes after exposure to H_2O_2. Ycf1–GFP also appeared as one or two dots on the vacuolar membrane, which are thought to be multivesicular bodies (MVBs) (C. M. Paumi, unpublished observation), in addition to the vacuolar membrane, but these puncta did not particularly increase upon exposure to H_2O_2 (Figure 8).

While the interaction between Rho1 and Ycf1 is clear from this study, Ycf1 is unlikely to be the only Rho1 effector involved in the oxidative stress response. Cells lacking *YCF1* exhibited little (or slight) hypersensitivity to hydrogen peroxide depending on H_2O_2 concentration. This could be due to the functional redundancy of other vacuolar membrane-residing transporters such as Ybt1 and Bpt1. However, none of the double or triple mutants of the vacuolar transporters was as sensitive as the *rho1^{ts}* mutants to H_2O_2 (M.-E. Lee, C. M. Paumi, and H.-O. Park, unpublished observation). Despite the lack of clear sensitivity of *ycf1*Δ to oxidants, a couple of observations suggest that the Rho1–Ycf1 interaction is significant to confer resistance to both metals and oxidants. The differential sensitivity of the *rho1^{ts}* mutants to paraquat and DEM is correlated with their sensitivity to cadmium (Figures 1 and 9A), which is well established as an inducer of oxidative stress in various cell types including yeast (Brennan and Schiestl 1996). A *ycf1* deletion confers an increased sensitivity of a *rho1^{ts}* mutant to H_2O_2 (Figure 9C).

The unique response of each *rho1^{ts}* mutant to various oxidants also suggests that the hypersensitivity to oxidants is unlikely due to the general sickness of the *rho1* mutants. This observation is consistent with the idea that different oxidants may trigger cellular responses by distinct mechanisms, as previously suggested (Thorpe *et al.* 2004). Hydrogen peroxide is an uncharged species (unlike superoxide, O_2^-) that penetrates membranes freely (Imlay 2008). While other oxidants such as diamide may affect the cell wall, H_2O_2 seems to affect the intracellular function (Vilella *et al.* 2005). We found that the *rho1-2* and *rho1-5* mutants, which are specifically defective in Pkc1 activation (Saka *et al.* 2001), were particularly hypersensitive to H_2O_2, but their sensitivities to other oxidants were opposite. Thus their hypersensitivity to H_2O_2 could be due in part to the defect in Pkc1 activation, but the role of the Pkc1–MAPK pathway in response to other oxidants seems less clear.

The *bck1*Δ and *mpk1/slt2*Δ mutants as examined here were mildly sensitive to H_2O_2. This is consistent with a previous report (Staleva *et al.* 2004), but differs from another study, which indicated that the *bck1* and *mpk1* mutants were not sensitive to H_2O_2 and diamide (Vilella *et al.* 2005). None of the *pkc1* mutants that we tested exhibited such severe sensitivity to H_2O_2, unlike the report by Vilella *et al.* (2005). This discrepancy might be due to the different *PKC1* alleles and the strain background. It is thus not certain whether the Pkc1–MAPK cascade plays a role under oxidative stress. The bifunctional transcription factor Skn7 might also be involved in the Rho1-mediated oxidative stress response (Alberts *et al.* 1998). Further investigation will be required to fully understand the mechanism by which Rho1 regulates the oxidative stress response.

In this study, we found that Rho1 is necessary for survival under oxidative stress. In contrast, Rho5 is necessary for cell death under excessive oxidative stress (Singh *et al.* 2008). Thus, despite the similar structure of these Rho GTPases, Rho1 and Rho5 seem to play opposite roles under oxidative stress. Cells may use an alternative program to promote either survival or death depending on the level of stress or cellular damage. It remains uncertain how cell fate is determined under different levels of oxidative stress. Although the details of the mechanism remain unknown, our findings suggest that Rho1 may regulate Ycf1 to get rid of heavy metals or other xenobiotics from the cytoplasm, and thus help yeast cells recover from oxidative stress. Because both Rho1 and Ycf1 belong to highly conserved families of proteins, Rho GTPases might also be involved in regulation of an ABC transporter in mammals.

Acknowledgments

We thank D. Levin, J. Gray, Y. Ohya, W. Guo, E. Bi, and W-K. Huh for providing strains and plasmids; K. Pan for help with image analysis; and P. J. Kang, L. Huang, and A. Simcox for discussion and comments on the manuscript. We are also grateful to M. Rose and the anonymous reviewers for insightful comments. This work was supported in part by research grants from the National Institutes of Health (NIH)/National Institute of General Medical Sciences (GM076375) and the American Heart Association to H.-O. P., and NIH/National Center for Research Resources (P20 RR020171) to C.M.P. The Stagljar lab is supported by grants from the Canadian Foundation for Innovation, the Canadian Institutes of Health Research, the Canadian Cancer Society Research Institute, the Heart and Stroke Foundation, the Cystic Fibrosis Foundation, the Ontario Genomics Institute, and Novartis.

Literature Cited

Alberts, A. S., N. Bouquin, L. H. Johnston, and R. Treisman, 1998 Analysis of RhoA-binding proteins reveals an interaction domain conserved in heterotrimeric G protein beta subunits and the yeast response regulator protein Skn7. J. Biol. Chem. 273: 8616–8622.

Ausubel, F. M., R. Brent, R. E. Kingston, D. D. Moore, J. G. Seidman *et al.*, 1999 *Current Protocols in Molecular Biology*. John Wiley & Sons, New York.

Avery, S. V., 2006 Microbial cell individuality and the underlying sources of heterogeneity. Nat. Rev. Microbiol. 4: 577–587.

Brennan, R. J., and R. H. Schiestl, 1996 Cadmium is an inducer of oxidative stress in yeast. Mutat. Res. 356: 171–178.

Cochemé, H. M., and M. P. Murphy, 2008 Complex I is the major site of mitochondrial superoxide production by paraquat. J. Biol. Chem. 283: 1786–1798.

Cohen, B. A., Y. Pilpel, R. D. Mitra, and G. M. Church, 2002 Discrimination between paralogs using microarray anal-

ysis: application to the Yap1p and Yap2p transcriptional networks. Mol. Biol. Cell 13: 1608–1614.
Cuypers, A., M. Plusquin, T. Remans, M. Jozefczak, E. Keunen *et al.*, 2010 Cadmium stress: an oxidative challenge. Biometals 23: 927–940.
Delley, P. A., and M. N. Hall, 1999 Cell wall stress depolarizes cell growth via hyperactivation of RHO1. J. Cell Biol. 147: 163–174.
Dong, Y., D. Pruyne, and A. Bretscher, 2003 Formin-dependent actin assembly is regulated by distinct modes of Rho signaling in yeast. J. Cell Biol. 161: 1081–1092.
Drgonova, J., T. Drgon, K. Tanaka, R. Kollar, G. C. Chen *et al.*, 1996 Rho1p, a yeast protein at the interface between cell polarization and morphogenesis. Science 272: 277–279.
Eitzen, G., N. Thorngren, and W. Wickner, 2001 Rho1p and Cdc42p act after Ypt7p to regulate vacuole docking. EMBO J. 20: 5650–5656.
Ercal, N., H. Gurer-Orhan, and N. Aykin-Burns, 2001 Toxic metals and oxidative stress part I: mechanisms involved in metal-induced oxidative damage. Curr. Top. Med. Chem. 1: 529–539.
Evangelista, M., K. Blundell, M. S. Longtine, C. J. Chow, N. Adames *et al.*, 1997 Bni1p, a yeast formin linking Cdc42p and the actin cytoskeleton during polarized morphogenesis. Science 276: 118–122.
Finkel, T., 2003 Oxidant signals and oxidative stress. Curr. Opin. Cell Biol. 15: 247–254.
Gasch, A. P., P. T. Spellman, C. M. Kao, O. Carmel-Harel, M. B. Eisen *et al.*, 2000 Genomic expression programs in the response of yeast cells to environmental changes. Mol. Biol. Cell 11: 4241–4257.
Godon, C., G. Lagniel, J. Lee, J.-M. Buhler, S. Kieffer *et al.*, 1998 The H2O2 stimulon in *Saccharomyces cerevisiae*. J. Biol. Chem. 273: 22480–22489.
Guo, W., F. Tamanoi, and P. Novick, 2001 Spatial regulation of the exocyst complex by Rho1 GTPase. Nat. Cell Biol. 3: 353–360.
Guthrie, C., and G. R. Fink, 1991 *Guide to Yeast Genetics and Molecular Biology.* Academic Press, San Diego.
Harrison, J. C., E. S. Bardes, Y. Ohya,, and D. J. Lew, 2001 A role for the Pkc1p/Mpk1p kinase cascade in the morphogenesis checkpoint. Nat. Cell Biol. 3: 417–420.
Harrison, J. C., T. R. Zyla, E. S. G. Bardes, and D. J. Lew, 2004 Stress-specific activation mechanisms for the "cell integrity" MAPK pathway. J. Biol. Chem. 279: 2616–2622.
He, X.-J., K. E. Mulford, and J. S. Fassler, 2009 Oxidative stress function of the *Saccharomyces cerevisiae* Skn7 receiver domain. Eukaryot. Cell 8: 768–778.
He, X. J., and J. S. Fassler, 2005 Identification of novel Yap1p and Skn7p binding sites involved in the oxidative stress response of *Saccharomyces cerevisiae*. Mol. Microbiol. 58: 1454–1467.
Herker, E., H. Jungwirth, K. A. Lehmann, C. Maldener, K.-U. Frohlich *et al.*, 2004 Chronological aging leads to apoptosis in yeast. J. Cell Biol. 164: 501–507.
Higgins, V. J., N. Alic, G. W. Thorpe, M. Breitenbach, V. Larsson *et al.*, 2002 Phenotypic analysis of gene deletant strains for sensitivity to oxidative stress. Yeast 19: 203–214.
Hu, C. D., Y. Chinenov, and T. K. Kerppola, 2002 Visualization of interactions among bZIP and Rel family proteins in living cells using bimolecular fluorescence complementation. Mol. Cell 9: 789–798.
Imlay, J. A., 2008 Cellular defenses against superoxide and hydrogen peroxide. Annu. Rev. Biochem. 77: 755–776.
Kamada, Y., U. S. Jung, J. Piotrowski, and D. E. Levin, 1995 The protein kinase C-activated MAP kinase pathway of *Saccharomyces cerevisiae* mediates a novel aspect of the heat shock response. Genes Dev. 9: 1559–1571.
Kang, P. J., L. Béven, S. Hariharan, and H.-O. Park, 2010 The Rsr1/Bud1 GTPase interacts with itself and the Cdc42 GTPase during bud-site selection and polarity establishment in budding yeast. Mol. Biol. Cell 21: 3007–3016.
Kang, P. J., A. Sanson, B. Lee, and H.-O. Park, 2001 A GDP/GTP exchange factor involved in linking a spatial landmark to cell polarity. Science 292: 1376–1378.
Kohno, H., K. Tanaka, A. Mino, M. Umikawa, H. Imamura *et al.*, 1996 Bni1p implicated in cytoskeletal control is a putative target of Rho1p small GTP binding protein in *Saccharomyces cerevisiae*. EMBO J. 15: 6060–6068.
Kono, K., S. Nogami, M. Abe, M. Nishizawa, S. Morishita *et al.*, 2008 G1/S cyclin-dependent kinase regulates small GTPase Rho1p through phosphorylation of RhoGEF Tus1p in *Saccharomyces cerevisiae*. Mol. Biol. Cell 19: 1763–1771.
Krause, S. A., and J. V. Gray, 2002 The protein kinase C pathway is required for viability in quiescence in *Saccharomyces cerevisiae*. Curr. Biol. 12: 588–593.
Lee, J., C. Godon, G. Lagniel, D. Spector, J. Garin *et al.*, 1999 Yap1 and Skn7 control two specialized oxidative stress response regulons in yeast. J. Biol. Chem. 274: 16040–16046.
Lee, K. S., and D. E. Levin, 1992 Dominant mutations in a gene encoding a putative protein kinase (BCK1) bypass the requirement for a *Saccharomyces cerevisiae* protein kinase C homolog. Mol. Cell. Biol. 12: 172–182.
Levin, D. E., 2005 Cell wall integrity signaling in *Saccharomyces cerevisiae*. Microbiol. Mol. Biol. Rev. 69: 262–291.
Levin, D. E., and E. Bartlett-Heubusch, 1992 Mutants in the S. cerevisiae PKC1 gene display a cell cycle-specific osmotic stability defect. J. Cell Biol. 116: 1221–1229.
Li, Z. S., Y. P. Lu, R. G. Zhen, M. Szczypka, D. J. Thiele *et al.*, 1997 A new pathway for vacuolar cadmium sequestration in *Saccharomyces cerevisiae*: YCF1-catalyzed transport of bis(glutathionato)cadmium. Proc. Natl. Acad. Sci. USA 94: 42–47.
Logan, M. R., L. Jones, and G. Eitzen, 2010 Cdc42p and Rho1p are sequentially activated and mechanistically linked to vacuole membrane fusion. Biochem. Biophys. Res. Commun. 394: 64–69.
López, E., C. Arce, M. J. Oset-Gasque, S. Cañadas, and M. P. González, 2006 Cadmium induces reactive oxygen species generation and lipid peroxidation in cortical neurons in culture. Free Radic. Biol. Med. 40: 940–951.
Mason, D. L., and S. Michaelis, 2002 Requirement of the N-terminal extension for vacuolar trafficking and transport activity of yeast Ycf1p, an ATP-binding cassette transporter. Mol. Biol. Cell 13: 4443–4455.
McCaffrey, M., J. S. Johnson, B. Goud, A. M. Myers, J. Rossier *et al.*, 1991 The small GTP-binding protein Rho1p is localized on the Golgi apparatus and post-Golgi vesicles in *Saccharomyces cerevisiae*. J. Cell Biol. 115: 309–319.
Morgan, B. A., G. R. Banks, W. M. Toone, D. Raitt, S. Kuge *et al.*, 1997 The Skn7 response regulator controls gene expression in the oxidative stress response of the budding yeast *Saccharomyces cerevisiae*. EMBO J. 16: 1035–1044.
Nagai, T., K. Ibata, E. S. Park, M. Kubota, K. Mikoshiba *et al.*, 2002 A variant of yellow fluorescent protein with fast and efficient maturation for cell-biological applications. Nat. Biotechnol. 20: 87–90.
Nguyên-nhu, N. T., and B. Knoops, 2002 Alkyl hydroperoxide reductase 1 protects *Saccharomyces cerevisiae* against metal ion toxicity and glutathione depletion. Toxicol. Lett. 135: 219–228.
Nonaka, H., K. Tanaka, H. Hirano, T. Fujiwara, H. Kohno *et al.*, 1995 A downstream target of RHO1 small GTP-binding protein is PKC1, a homolog of protein kinase C, which leads to activation of the MAP kinase cascade in *Saccharomyces cerevisiae*. EMBO J. 14: 5931–5938.
Obrdlik, P., M. El-Bakkoury, T. Hamacher, C. Cappellaro, C. Vilarino *et al.*, 2004 K+ channel interactions detected by a genetic sys-

tem optimized for systematic studies of membrane protein interactions. Proc. Natl. Acad. Sci. USA 101: 12242–12247.
Park, H.-O., and E. Bi, 2007 Central roles of small GTPases in the development of cell polarity in yeast and beyond. Microbiol. Mol. Biol. Rev. 71: 48–96.
Park, H.-O., J. Chant, and I. Herskowitz, 1993 *BUD2* encodes a GTPase-activating protein for Bud1/Rsr1 necessary for proper bud-site selection in yeast. Nature 365: 269–274.
Park, J.-I., E. J. Collinson, C. M. Grant, and I. W. Dawes, 2005 Rom2p, the Rho1 GTP/GDP exchange factor of *Saccharomyces cerevisiae*, can mediate stress responses via the Ras-cAMP pathway. J. Biol. Chem. 280: 2529–2535.
Paumi, C. M., J. Menendez, A. Arnoldo, K. Engels, K. R. Iyer *et al.*, 2007 Mapping protein-protein interactions for the yeast ABC transporter Ycf1p by integrated split-ubiquitin membrane yeast two-hybrid analysis. Mol. Cell 26: 15–25.
Qadota, H., C. P. Python, S. B. Inoue, M. Arisawa, Y. Anraku *et al.*, 1996 Identification of yeast Rho1p GTPase as a regulatory subunit of 1,3-beta-glucan synthase. Science 272: 279–281.
Saka, A., M. Abe, H. Okano, M. Minemura, H. Qadota *et al.*, 2001 Complementing yeast rho1 mutation groups with distinct functional defects. J. Biol. Chem. 276: 46165–46171.
Sharma, K. G., D. L. Mason, G. Liu, P. A. Rea, A. K. Bachhawat *et al.*, 2002 Localization, regulation, and substrate transport properties of Bpt1p, a *Saccharomyces cerevisiae* MRP-type ABC transporter. Eukaryot. Cell 1: 391–400.
Singh, K., P. J. Kang, and H.-O. Park, 2008 The Rho5 GTPase is necessary for oxidant-induced cell death in budding yeast. Proc. Natl. Acad. Sci. USA 105: 1522–1527.
Snider, J., S. Kittanakom, D. Damjanovic, J. Curak, V. Wong *et al.*, 2010 Detecting interactions with membrane proteins using a membrane two-hybrid assay in yeast. Nat. Protoc. 5: 1281–1293.
Staleva, L., A. Hall, and S. J. Orlow, 2004 Oxidative stress activates FUS1 and RLM1 transcription in the yeast *Saccharomyces cerevisiae* in an oxidant-dependent manner. Mol. Biol. Cell 15: 5574–5582.
Thorpe, G. W., C. S. Fong, N. Alic, V. J. Higgins, and I. W. Dawes, 2004 Cells have distinct mechanisms to maintain protection against different reactive oxygen species: oxidative-stress-response genes. Proc. Natl. Acad. Sci. USA 101: 6564–6569.
Valko, M., H. Morris, and M. T. Cronin, 2005 Metals, toxicity and oxidative stress. Curr. Med. Chem. 12: 1161–1208.
Vida, T. A., and S. D. Emr, 1995 A new vital stain for visualizing vacuolar membrane dynamics and endocytosis in yeast. J. Cell Biol. 128: 779–792.
Vilella, F., E. Herrero, J. Torres, and M. A. de la Torre-Ruiz, 2005 Pkc1 and the upstream elements of the cell integrity pathway in *Saccharomyces cerevisiae*, Rom2 and Mtl1, are required for cellular responses to oxidative stress. J. Biol. Chem. 280: 9149–9159.
Wemmie, J. A., and W. S. Moye-Rowley, 1997 Mutational analysis of the *Saccharomyces cerevisiae* ATP-binding cassette transporter protein Ycf1p. Mol. Microbiol. 25: 683–694.
Yoshida, S., K. Kono, D. M. Lowery, S. Bartolini, M. B. Yaffe *et al.*, 2006 Polo-like kinase Cdc5 controls the local activation of Rho1 to promote cytokinesis. Science 313: 108–111.
Yoshida, S., S. Bartolini, and D. Pellman, 2009 Mechanisms for concentrating Rho1 during cytokinesis. Genes Dev. 23: 810–823.

Communicating editor: M. D. Rose

GENETICS

Supporting Information
http://www.genetics.org/content/suppl/2011/05/30/genetics.111.130724.DC1

The Rho1 GTPase Acts Together With a Vacuolar Glutathione S-Conjugate Transporter to Protect Yeast Cells From Oxidative Stress

Mid Eum Lee, Komudi Singh, Jamie Snider, Archana Shenoy, Christian M. Paumi, Igor Stagljar, and Hay-Oak Park

DOI: 10.1534/genetics.111.130724

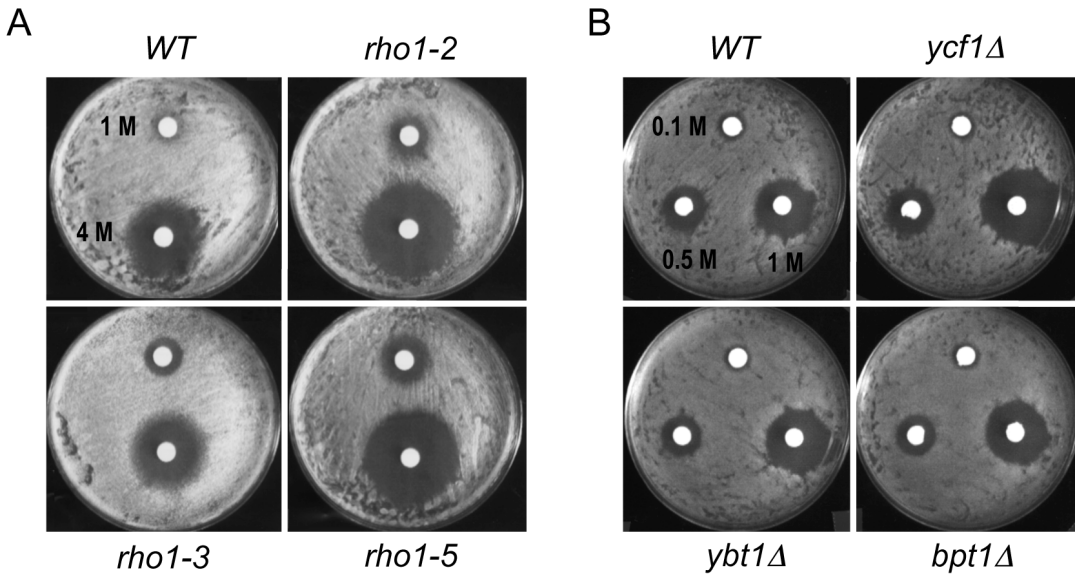

Figure S1 Sensitivity of the *rho1*^{ts} mutants and the vacuolar transporter mutants to H_2O_2.

A. H_2O_2 sensitivity of wild type (NY2284) and *rho1*^{ts} mutants (NY2285-NY2287) were tested by halo assays on YPD plates as described in Materials and Methods. The plates were incubated at 30°C for 2 d.
B. H_2O_2 sensitivity of wild type (BY4741) and isogenic deletion mutants of vacuolar transporters (*ycf1Δ*, *ybt1Δ* and *bpt1Δ*) was tested by halo assays on SC plates. The plates were incubated at 30°C for 2 d.

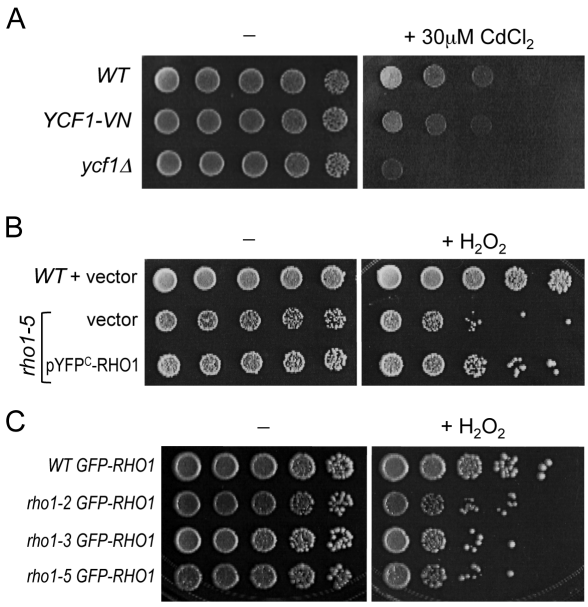

FIGURE S2 Ycf1 and Rho1 fusions are partially functional.

A. *YCF1-VN* partially complemented hypersensitivity of an *ycf1Δ* mutant to cadmium. Five-fold serial dilutions (from left to right, starting from OD_{600} = 2) of wild-type (NY2284), *YCF1-VN* (HPY1710) and *ycf1Δ* (HPY1738) were grown in SC, spotted on SC plate (-) or SC plate containing 30 μM $CdCl_2$, and then incubated for 4 d at room temperature.

B. A low-copy YFPC-Rho1 plasmid partially complemented hypersensitivity of *rho1-5* to H_2O_2. 2.5-fold serial dilutions (from left to right, starting from OD_{600} = 0.4) of wild-type (NY2284) and *rho1-5* (NY2287) cells carrying pRS316 (vector) or pRS316-YFPC-Rho1 (pHP1765) were treated with 1 mM H_2O_2 for 200 min, spotted on SC-Ura and then incubated for 3 d at 30°C.

C. GFP-Rho1 partially complemented hypersensitivity of the *rho1*^{ts} mutants to oxidants. Five-fold serial dilutions (from left to right, starting from OD_{600}= 0.8) of wild-type (HPY1574), *rho1-2* (HPY1730), *rho1-3* (HPY1731) and *rho1-5* (HPY1732) mutants expressing GFP-Rho1 from the chromosome were treated with 3 mM H_2O_2 for 200 min, spotted on YPD and then incubated for 3 d at 30°C.

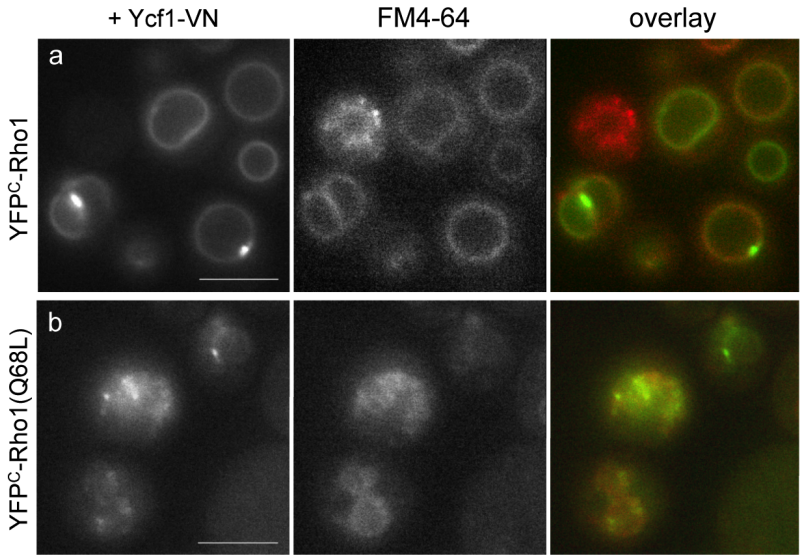

Figure S3 Localization of the Rho1-Ycf1 or Rho1^{Q68L}-Ycf1 bimolecular fluorescent complex in cells stained with FM4-64. BiFC assays were performed in wild-type cells (HPY1710), which co-express Ycf1-VN from the chromosome and (a) YFP^{C}-Rho1 or (b) YFP^{C}-Rho1^{Q68L} from a plasmid, after staining with FM4-64. Cells were grown in SC-URA at 30^{o}C. Images were captured with the YFP filter for 8 sec exposure and TRITC filter for 200 msec. Bars, 5 μm.

File S1

Construction of Plasmids and Strains

Yeast strains and plasmids used in this study are listed in Table 1 and Table S1, respectively.

Plasmids and strains for GFP-Rho1: To construct a plasmid for GFP-Rho1 expression, first, *Not*I site was introduced just after the start codon of *RHO1* as follows: The 685-bp DNA fragment covering the region upstream of the start codon was amplified by PCR using YEp24-RHO1 (OZAKI *et al.* 1996) as template and primers oRHO13 (5'-GAACAAGCTTCTCCCTAT AATGCGGTAGCATTGG-3') and oRHO18 (5'-GAAGGCGGCCGCACATCTTTCTAGTATAATTTTTAAAGTTC-3'). In addition, a 1.23-kb fragment covering the *RHO1* ORF from the start codon was amplified by PCR using primers oRHO16 (5'-GAAGCTCGAGCCACCAGGGTTTATCAATGCTCGC-3') and oRHO17 (5'-GAACGCGGCCGCTCACAACAAGTTGG TAACAGTATC-3'). After digestion of the 685-bp fragment with *Hind*III and *Not*I (sites included in the primers) and the 1.23-kb fragment with *Not*I and *Xho*I (sites included in the primers), these two fragments were cloned into the pRS426* (pHP1476 = pRS426 lacking *Not*I) (SINGH *et al.* 2008) digested with *Hind*III and *Xho*I, yielding pRS426* -RHO1 (pHP1697). Next, a 720-bp *Not*I fragment encoding $GFP^{S65T, V163A, S175G}$, isolated from YCp-GFP-RSR1 (pHP767) (PARK *et al.* 2002), was inserted into the *Not*I site of pHP1697, yielding pRS426*-GFP-RHO1 (pHP1698). The correct orientation of the GFP insertion in pHP1698 was confirmed by digestion with *Pvu*II.

To construct an integrating plasmid pRS306-GFP-RHO1, pHP1698 was digested with *Hind*III and *Xho*I, and the resulting 2.6-kb fragment containing the *GFP-RHO1* sequence was cloned into pRS306 (SIKORSKI and HIETER 1989) digested with *Hind*III and *Xho*I, yielding pRS306-GFP-RHO1 (pHP1699). To express GFP-Rho1 from the chromosome, pHP1699 was linearized with *Bgl*II (which is located at 420 bp downstream of the stop codon of the *RHO1* ORF) and integrated into the appropriate strains (see Table 1), and then stable integrants were isolated.

Plasmids and Yeast Strains for BiFC: To construct a strain expressing *YCF1* tagged with the N-terminal fragment of Venus (VN) at the C-terminus, a DNA fragment carrying VN-kanMX6 was amplified by PCR using pFA6a-VN-KanMX6 (SUNG and HUH 2007) as template and primers oYCF11 (5'-TTGTTCTATTCACTGTGCATGGAGGCTGGTTTGGTCAATGAAAAT CGGATCCCCGGGTTAATTAA-3') and oYCF12 (5'-CTACGTACCAGATTGTGCGGGACAGGTTTTTATTAGTTTC ACAGTGAATTCGAGCTCGTTTAAAC-3'). The resulting PCR product was transformed into NY2284 by one-step-replacement method (ROTHSTEIN 1991), yielding HPY1710. Correct targeting was confirmed by colony PCR using primers oYCF13 (5'-AGCCGAGTTTGACTCTCCGGGCCAG-3') and oYCF14 (5'-GCACCTGTTCTCCGGAGAAATGTTG-3').

To express Rho1 fused to the C-terminal fragment of YFP (YFP^C) at its N terminus, first, the 252 bp *Not*I fragment of YFP^C generated from pRS304-YFP^C-$RSR1^{K16N}$ (pHP1678) (KANG *et al.* 2010) was cloned into the *Not*1 site of pRS426*-RHO1 (pHP1697),

yielding pRS426*-YFP^{C}-RHO1 (pHP1737). To express YFP^{C}-Rho1 from a CEN plasmid, the 2.1 kb *Hind*III -*Xho*I fragment (carrying YFP^{C}-RHO1 sequence) from pHP1737 was cloned into pRS316 digested with *Hind*III and *Xho*I, yielding pRS316-YFP^{C}-RHO1 (pHP1765).

The *RHO1*^{Q68L} and the *RHO1*^{T24N} mutations were generated by PCR-based site-directed mutagenesis using pHP1737 as template and primer pairs oRHO19 (5'-GCGCTATGGGATACCGCTGGTCTAGAAGATTATGAT AGACTAAG-3') and oRHO110 (5'-CTTAGTCTATCATAATCTTCTAGACCAGCGGTATCCCATAGCGC-3'); and oRHO111 (5'-GGTGATG GTGCCTGTGGTAAGAACTGTTTATTAATCGTCTTTTCCAAGGGC-3') and oRHO112 (5'-GCCCTTGGAAAAGAC GATTAATAAACAGTTCTTACCACAGGCACCATCACC-3'), yielding pRS426-YFP^{C}-RHO1^{Q68L} (pHP1744) and pRS426-YFP^{C}-RHO1^{T24N} (pHP1745), respectively. The correct mutations were confirmed by DNA sequencing. To express *RHO1*^{Q68L} and *RHO1*^{T24N} from CEN plasmids, pRS316-YFP^{C}-RHO1^{Q68L} (pHP1766) and pRS316-YFP^{C}-RHO1^{T24N} (pHP1768) were generated from pHP1744 and pHP1745, respectively, as described above.

To construct *TUS1* deletion in the strain HPY1710, PCR was performed using pFA6a-TRP1 (LONGTINE *et al.* 1998) as template and primer pairs, oTUS15 (5'-CGAATATAAACATTAAAACAAAAAACTTATTGAGTGCAGCAAGTTAACC GGATCCCCGGGTTAATTAA-3') and oTUS16 (5'-TTATATTATTACAACGATATTTACCATTAAAAGTGTCTATAT CTTATAGAATTCGAGCTC GTTTAAAC-3'). The resulting PCR product was used to delete the chromosomal *TUS1* gene in HPY1710 by one-step gene disruption (ROTHSTEIN 1991), yielding HPY1737. Correct targeting was confirmed by colony PCR using primer pairs, oTUS17 (5'-CATACTGACTCGTCGCATAGGCCG-3') and oTRP11 (5'-GTTCACCTGTCCCACCTG CTTCTG-3').

Plasmids and Strains for Integrated Membrane Yeast Two-Hybrid (iMYTH): iMYTH construct generation and assays were carried out as previously described (PAUMI *et al.* 2007; SNIDER *et al.* 2010) using four THY AP4 MYTH reporter strains—YCF1-CT expressing the C-terminally Cub-LexA-VP16 tagged Ycf1; ArBT-CT expressing Cub-LexA-VP16 tagged artificial bait control construct comprised of the yeast mating factor alpha signal sequence ('MFαSS') fused to the transmembrane domain of the human T-cell surface glycoprotein CD4 ('CD4tm'); and two *tus1Δ* strains, YCF1-CT ΔT and ArBT-CT ΔT, derived from YCF1-CT and ArBT-CT, respectively. To construct the *TUS1* deletion strains in the MYTH bait backgrounds, the NatR resistance cassette was amplified by PCR using primers containing 5' region homologous to 45 bp upstream ('forward' primer) or downstream ('reverse' primer) of the *TUS1* gene. This PCR product, consisting of the NatR cassette flanked on either side by sequence homologous to the *TUS1* gene region, was used to delete the *TUS1* gene by one-step gene disruption (ROTHSTEIN 1991).

Construction of Rho1 prey constructs was carried out as follows. The *RHO1* gene was amplified from purified *Saccharomyces cerevisiae* genomic DNA and cloned into either the pPR3N or pPR3C MYTH prey vectors (Dualsystems Biotech)

using the classical 'gap-repair' homologous recombination method in yeast (MA *et al.* 1987). For pPR3N cloning, PCR was carried out using the R3NF (5'-atccaagcagtggtatcaacgcagagtggccattacggccATGTCACAACAAGTTGGTAACAGTATC-3') and R3NR (5'-tacatgactcgaggtcgacggtatcgataagcttgatatcCTATAACAAGACACACTTCTTCTTC-3') primers. For pPR3C cloning, the R3CF (5'-gcacaatatttcaagctataccaagcatacaatcaactcAACACAATGTCACAACAAGTTGGTAACAGTATC-3') and R3CR (5'-gcttgatatcgaattctcgagaggccgaggcggccgacatTAACAAGACACACTTCTTCTTCTTC-3') primers were used.

Construction of *ycf1* deletion mutants and the *YCF1-GFP* strain: To construct *YCF1* deletion in the NY2284 background, a DNA fragment (2.08 kb) carrying *ycf1Δ::KanMX4* was amplified by colony PCR using HPY1904 (an *ycf1Δ*:: KanMX4 strain obtained from Open Biosystems) and primers, oYCF15 (5'-CTCCTGGTGTGATGCTTGGGCGGTG-3') and oYCF14 (5'-GCACCTGTTCTCCGGAGAAATGTTG-3'). The resulting PCR product was used to delete the chromosomal *YCF1* gene in NY2284 and NY2287 by one-step gene disruption (ROTHSTEIN 1991), yielding HPY1738 and HPY1739, respectively. Colony PCR was performed using primers oYCF14 and oKanC (5'-CGAGTGATTTTGATGACGAGCGTA ATGGCTGG-3') to confirm the correct deletion, which generated a 0.8-kb DNA fragment. The phenotype of *ycf1Δ* was confirmed by checking growth on a plate containing 30 μM $CdCl_2$.

To construct a strain expressing Ycf1 fused to GFP at its C terminus, a DNA fragment encoding GFP-TRP1 was amplified by PCR using pFA6a-GFP(S65T)-TRP1 (LONGTINE *et al.* 1998) as template and primers oYCF11 and oYCF12. The resulting PCR product was transformed into NY2284 by one-step-replacement method, yielding HPY1955. Correct targeting was confirmed by colony PCR using primers oYCF13 and oTRP11.

Table S1 Plasmids used in this study

Plasmid	Description	Source/Comments
pRS426	*URA3* (high copy)	(CHRISTIANSON *et al.* 1992)
pRS316	*URA3* (CEN)	(SIKORSKI and HIETER 1989)
pRS306	*URA3* (integrative)	(SIKORSKI and HIETER 1989)
pFA6a-TRP1		(LONGTINE *et al.* 1998)
pFA6a-GFP(S65T)-TRP1		(LONGTINE *et al.* 1998)
pFA6a-VN-KanMX6		(SUNG and HUH 2007)
pHP767	YCp50-GFP-BUD1	(PARK *et al.* 2002)
pHP1409	YEp24-RHO1	(OZAKI *et al.* 1996)
pHP1476	pRS426 lacking *Not*I (= pRS426*)	(SINGH *et al.* 2008)
pHP1697	pRS426*-RHO1 with *Not*I site right after ATG	This study
pHP1698	pRS426*-GFP-RHO1	This study
pHP1699	pRS306-GFP-RHO1	This study
pHP1678	pRS304-YFP^{C}-RSR1^{K16N}	(KANG *et al.* 2010)
pHP1730	YCp50-YFP^{C}-rsr1	(KANG *et al.* 2010)
pHP1737	pRS426*-YFP^{C}-RHO1	This study
pHP1744	pRS426*-YFP^{C}-RHO1^{Q68L}	This study
pHP1745	pRS426*-YFP^{C}-RHO1 ^{T24N}	This study
pHP1765	pRS316-YFP^{C}-RHO1	This study
pHP1766	pRS316-YFP^{C}-RHO1^{Q68L}	This study
pHP1768	pRS316-YFP^{C}-RHO1^{T24N}	This study
pPR3-N	2 micron, *TRP1*, Amp^{R}, NubG	(SNIDER *et al.* 2010)
pPR3-C	2 micron, *TRP1*, Amp^{R}, NubG	(SNIDER *et al.* 2010)

LITERATURE CITED

CHRISTIANSON, T. W., R. S. SIKORSKI, M. DANTE, J. H. SHERO and P. HIETER, 1992 Multifunctional yeast high-copy-number shuttle vectors. Gene **110:** 119-122.

KANG, P. J., L. BEVEN, S. HARIHARAN and H.-O. PARK, 2010 The Rsr1/Bud1 GTPase Interacts with Itself and the Cdc42 GTPase during Bud-Site Selection and Polarity Establishment in Budding Yeast. Mol. Biol. Cell **21:** 3007-3016.

LONGTINE, M. S., A. I. MCKENZIE, D. J. DEMARINI, N. G. SHAH, A. WACH *et al.*, 1998 Additional modules for versatile and economical PCR-based gene deletion and modification in *Saccharomyces cerevisiae*. Yeast **14:** 953-961.

MA, H., S. KUNES, P. J. SCHATZ and D. BOTSTEIN, 1987 Plasmid construction by homologous recombination in yeast. Gene **58:** 201-216.

OZAKI, K., K. TANAKA, H. IMAMURA, T. HIHARA, T. KAMEYAMA *et al.*, 1996 Rom1p and Rom2p are GDP/GTP exchange proteins (GEPs) for the Rho1p small GTP binding protein in *Saccharomyces cerevisiae*. EMBO J. **15:** 2196-2207.

PARK, H.-O., P. J. KANG and A. W. RACHFAL, 2002 Localization of the Rsr1/Bud1 GTPase involved in selection of a proper growth site in yeast. J. Biol. Chem. **277:** 26721-26724.

PAUMI, C. M., J. MENENDEZ, A. ARNOLDO, K. ENGELS, K. R. IYER *et al.*, 2007 Mapping protein-protein interactions for the yeast ABC transporter Ycf1p by integrated split-ubiquitin membrane yeast two-hybrid analysis. Mol. Cell **26:** 15-25.

ROTHSTEIN, R., 1991 Targeting, disruption, replacement, and allele rescue: Integrative DNA transformation in yeast. Methods Enzymol **194:** 281-301.

SIKORSKI, R. S., and P. HIETER, 1989 A system of shuttle vectors and yeast host strains designed for efficient manipulation of DNA in *Saccharomyces cerevisiae*. Genetics **122:** 19-27.

SINGH, K., P. J. KANG and H.-O. PARK, 2008 The Rho5 GTPase is necessary for oxidant-induced cell death in budding yeast. Proc. Natl. Acad. Sci. USA. **105:** 1522-1527.

SNIDER, J., S. KITTANAKOM, D. DAMJANOVIC, J. CURAK, V. WONG *et al.*, 2010 Detecting interactions with membrane proteins using a membrane two-hybrid assay in yeast. Nat. Protoc. **5:** 1281-1293.

SUNG, M.-K., and W.-K. HUH, 2007 Bimolecular fluorescence complementation analysis system for *in vivo* detection of protein-protein interaction in *Saccharomyces cerevisiae*. Yeast **24:** 767-775.